



**HAL**  
open science

## On the similarity of plastic flow processes during smooth and jerky flow in dilute alloys

M.A. Lebyodkin, N.P. P Kobelev, Y. Bougherira, Denis Entemeyer, C. Fressengeas, T.A. A Lebedkina, I.V. V Shashkov

### ► To cite this version:

M.A. Lebyodkin, N.P. P Kobelev, Y. Bougherira, Denis Entemeyer, C. Fressengeas, et al.. On the similarity of plastic flow processes during smooth and jerky flow in dilute alloys. *Acta Materialia*, 2012, 60 (3), pp.844-850. 10.1016/j.actamat.2011.10.042 . hal-02173961

**HAL Id: hal-02173961**

**<https://hal.science/hal-02173961>**

Submitted on 21 Jul 2019

**HAL** is a multi-disciplinary open access archive for the deposit and dissemination of scientific research documents, whether they are published or not. The documents may come from teaching and research institutions in France or abroad, or from public or private research centers.

L'archive ouverte pluridisciplinaire **HAL**, est destinée au dépôt et à la diffusion de documents scientifiques de niveau recherche, publiés ou non, émanant des établissements d'enseignement et de recherche français ou étrangers, des laboratoires publics ou privés.

# On the similarity of plastic flow processes during smooth and jerky flow in dilute alloys

M.A. Lebyodkin<sup>a</sup>, N. P. Kobelev<sup>b</sup>, Y. Bougherira<sup>a</sup>, D. Entemeyer<sup>a</sup>, C. Fressengeas<sup>a</sup>,  
T.A. Lebedkina<sup>b</sup>, I.V. Shashkov<sup>a,b</sup>

<sup>a</sup>*LEM3 (Laboratoire d'Etude des Microstructures et de Mécanique des Matériaux), Université Paul Verlaine-Metz, CNRS UMR 7239, Ile du Saulcy, 57045 Metz, France*

<sup>b</sup>*Institute of Solid State Physics RAS, 142432 Chernogolovka, Russia*

**Abstract.** The jerky flow of dilute alloys, or the Portevin–Le Chatelier effect, has a burst-like intermittent character at different fluctuation size levels. Multifractal analysis is applied to both the macroscopic stress serrations and the acoustic emission accompanying the plastic deformation. Multifractal scaling is found for both kinds of time series. The scaling range of the stress serrations is limited from below by their characteristic frequency. Unexpectedly, the scaling range for acoustic bursts not only covers this range but spreads to much shorter time scales with the same scaling exponent. This result testifies that the deformation processes revealed by the acoustic emission at a mesoscopic scale have a similar nature during both stress serrations and smooth plastic flow. The implications on the crossovers in the dynamics of jerky flow are discussed.

*Keywords:* Portevin-Le Chatelier effect; Acoustic methods; Dynamic phenomena; Self-organization; Synchronization.

---

## 1. Introduction

Jerky flow, or the Portevin–Le Chatelier (PLC) effect, has been lately attracting attention as a phenomenon caused by the collective dynamics of the complex system formed by crystal defects – dislocations and solute atoms [1–8]. Its mechanism is usually ascribed to dynamic strain aging: when the dislocations are arrested at obstacles during the waiting time necessary for thermal activation of their motion, diffusing solute atoms lead to their additional pinning followed by abrupt break-away. The onset of plastic instability usually occurs after macroscopically uniform deformation to a certain critical strain  $\varepsilon_{cr}$ . In conventional tensile tests with a constant imposed overall strain rate,  $\dot{\varepsilon}_a$ , the plastic strain rate becomes localized within the so-called PLC deformation bands, whose formation leads to stress serrations. At a given temperature, the instability is observed in an applied strain-rate range determined by the balance between the corresponding waiting time and the characteristic time for the diffusion of solute atoms. Close to the

upper bound of this interval, the PLC bands continuously propagate along the specimen, with irregular stress fluctuations (type A behavior). Relay-race propagation of PLC bands (type B) or almost uncorrelated static bands (type C), both behaviors associated with deep stress drops with a characteristic size, are observed at intermediate and low  $\dot{\epsilon}_a$  values, respectively. Application of various statistical and time series analyses to the stress–time curves uncovered different and complex correlation regimes between the stress serrations, depending on the driving strain rate. In particular, a scale-free behavior in terms of power-law statistical distributions of the stress drop size and duration was found for type A instability in AlMg [1,4] and CuAl [3] alloys. This observation led to a conjecture of self-organized critical behavior [9], while deterministic chaos [10] and near-Gaussian statistical distributions of stress drops were detected for type B serrations in similar alloys [2–4]. Multifractal scaling was found for stress–time curves in the entire strain-rate range of instability [4,11].

The acoustic emission (AE) technique allows burst-like plastic activity to be detected, even when the traditionally measured deformation curves show smooth behavior which was for a long time considered to result from stochastic movements of dislocations. Until lately, the multifractal and dynamic analyses referred to above were not carried out for AE studies of plastic flow, except for recent multifractal analysis of isolated AE bursts during the PLC effect [8]. Only the statistical analysis was used for the macroscopically smooth deformation of pure materials (e.g. Ref.[12]). In Ref. [13], the statistical analysis was applied to study AE series during plastic deformation of an AlMg alloy. Power-law distributions of the amplitudes of AE events were found in Ref.[13] in all experimental conditions: both below and beyond  $\epsilon_{cr}$ , at high as well as at low strain rates. These observations suggest scale-invariant avalanche-like nature of the deformation processes in a range of fluctuation size pertaining to the AE, a conjecture consistent with the data for pure materials [12], as well as with the observations of power-law statistics for the tiny stress serrations occurring on the deformation curves of nanopillars [14]. However, what is specific to the PLC investigation is that, except for the high  $\dot{\epsilon}_a$  limit (and for reasons not linked with finite sample size), scale invariance is broken at the larger scale of the macroscopic stress serrations accompanying plastic instability. An attempt at understanding the relationships between the different fluctuation scales of the plasticity processes during the PLC instability is therefore undertaken in the present work, by using the multifractal analysis of both the deformation curves and the accompanying AE. Indeed, the above statistical distributions only characterize the probability of occurrence of plastic activity with a given intensity during the test duration, but they do not provide the information on the relative arrangement of the plastic events. The multifractal analysis has the advantage of uncovering the

presence of correlations and characterizing their scaling properties, although it does not handle the information on the location of the corresponding events (see e.g. Ref. [11]).

The paper is organized as follows. Sections 2 and 3 describe the experimental setup and outline the implementation of the multifractal approach to the analysis of the AE and stress time series. Section 4 presents the experimental observations and the results of the data analysis. It is concluded that both kinds of time series are characterized by long-range correlations leading to multifractal behavior in certain time-scale ranges. The discussion from the viewpoint of the underlying physical mechanisms governing the collective dislocation dynamics is given in Section 5.

## 2. Experimental technique

Dog-bone-shaped specimens with a gauge part  $25 \times 6.8 \times 2.5 \text{ mm}^3$  in size were cut from a cold-rolled sheet of polycrystalline Al3% Mg alloy, annealed at  $400^\circ\text{C}$  for 2 h, and quenched into water. Tensile tests were conducted at room temperature with a constant cross-head velocity corresponding to a wide  $\dot{\epsilon}_a$  range covering all the above-mentioned behaviors:  $2 \times 10^{-5} \text{ s}^{-1}$ ,  $6.7 \times 10^{-5} \text{ s}^{-1}$ ,  $2 \times 10^{-4} \text{ s}^{-1}$ ,  $6 \times 10^{-4} \text{ s}^{-1}$ , and  $6 \times 10^{-3} \text{ s}^{-1}$ . The sampling time used to record the entire stress–time curves was chosen as a function of  $\dot{\epsilon}_a$ , similar to Ref. [4], and was equal to 500 ms, 100 ms, 20 ms, 4 ms, and 4 ms, respectively. Besides, shorter portions of low strain-rate curves were recorded with the sampling time of 20 ms. The precision of the load measurement corresponded to at least 0.01 MPa stress accuracy for the above specimens. Three to six tests were conducted for each strain rate. A computer-controlled Physical Acoustics LOCAN 320 system was used to record the AE captured by a piezoelectric transducer with a frequency band of 100–600 kHz. The transducer was clamped to the greased surface just above the deforming part of the sample. The sampling rate of the recording system was 4 MHz. It should be specified that such equipment does not record the AE signal “continuously” at the given sampling time, but picks out acoustic events exceeding a pre-set threshold voltage and measures their characteristics, such as amplitude, duration, count rate, energy, and so on. Its total gain and the threshold voltage for the identification of the starting point of an AE event were respectively 80 dB and 27 dB. The latter value corresponds to the acoustic noise of the free-running deforming machine. The discrimination of the AE events was based on a conventional procedure; namely, the event is considered to come to an end if the acoustic signal remains below the threshold voltage for a period exceeding a pre-set value called hit definition time (HDT). The event is followed by a certain dead time, during which no measurement is performed in order to filter out sound reflections. In the present work, both time windows were set at 300  $\mu\text{s}$ , or ten times less in control tests.

### 3. Data processing

In order to ensure continuity with previous analyses of stress–time curves, a similar procedure of the multifractal (MF) analysis was applied (see e.g. Refs. [4,15–17]). More specifically, the slow trend caused by the work hardening of the material is first removed from the  $\sigma(t)$  curve using one of the normalization methods proposed in Refs. [1,4,15] for various shapes of serrated curves. The analysis is then applied to the time series  $\psi_k$ , which is given by the absolute value of the stress time derivative and, as suggested in Ref.[4], reflects bursts of the plastic activity. The choice of the AE time series deserves some explanation. It is well known that the duration of the AE events and related characteristics, such as the acoustic energy or the average count rate, display bursts which are strongly correlated with the type B or type C stress serrations and surpass the average level of the respective signal by orders of magnitude [18,19]. Consequently, the overall set of events displays two distinct scale ranges. Preliminary analysis of the data obtained demonstrated that the bursts prevail in the statistical or multifractal properties of the corresponding time series at low and intermediate strain rate and lead to the results similar to those for the series of stress drops. Particularly, bell-shaped statistical distributions were found in these conditions, in contrast to the scale-invariant distributions of the amplitudes of AE events [13]. A new insight was provided by the multifractal analysis of the time series represented by the sequence of amplitudes of the AE events, related to the instants when the events occur (see bottom pictures in Figs. 1 and 2). The details of such investigation are addressed in the present paper.

By covering the total time interval  $T$  with a grid of  $N$  intervals  $\delta t$ , a local probabilistic measure  $\mu_i(\delta t)$  of the corresponding signal in the  $i$ th interval is defined as the sum of the  $\psi_k$  values within it, normalized by their total sum. The scaling properties of the partition functions  $S_q = \sum_{i=1}^N \mu_i^q$ , where  $q$  is a real number, are then studied with regard to  $\delta t$ . Obviously, only nonempty intervals corresponding to non zero measure are present in these sums. If the time series has a self-similar character,  $S_q$  is proportional to  $\delta t^{(q-1)D_q}$ , where the generalized fractal dimensions  $D_q$  depend on  $q$ . In particular, the trivial relationship,  $D_q \equiv 1$ , should be found in the case of random behavior. Essentially, the multifractal analysis allows uncovering the presence of correlations between both amplitudes and times of occurrence of events in the signal through their scaling behavior, and characterizing the heterogeneity of the scaling properties over a range of subsets of events. Focusing on a given subset is obtained through the choice of  $q$ : for example, large positive  $q$ -values tend to select large measures in the partition function, while large negative  $q$ -values allow highlighting small events. Variation of  $q$  over a set of real numbers thus provides continuous characterization of heterogeneity. Some of the  $D_q$  values have clear sense:  $D_0$ ,  $D_1$ , and  $D_2$  are the

capacity, information, and correlation dimensions, respectively [20]. A wide spectrum of  $D_q$  values indicates a substantial shift in the correlation characteristics between large events on the one hand, and small events on the other hand. Note that most natural fractals are multifractals, since (homogeneous) fractality is a more demanding property than (heterogeneous) multifractality.

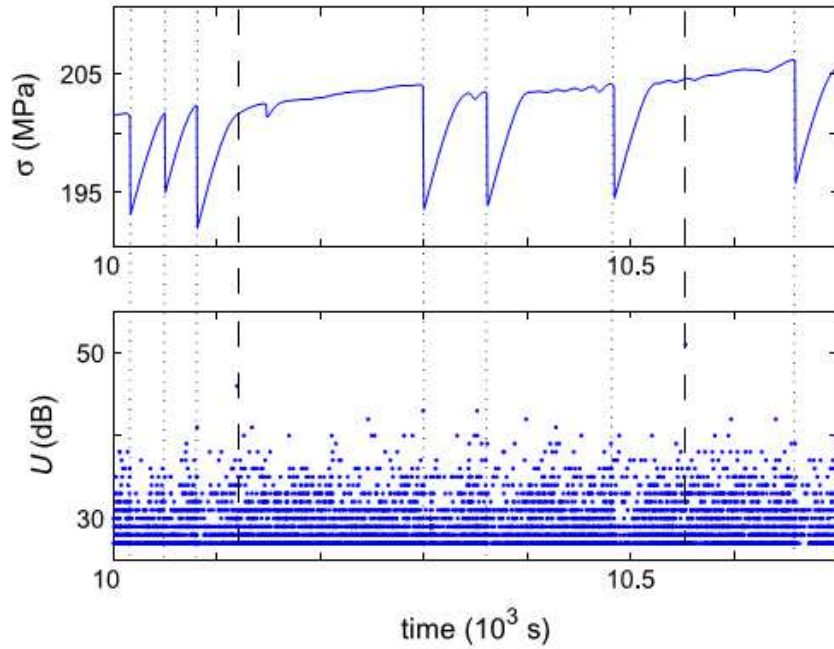


**Fig. 1.** Blow up of parts of a deformation curve  $\sigma(t)$  and the accompanying AE signal  $U(t)$  for the least value of the imposed strain rate,  $\dot{\epsilon}_a = 2 \times 10^{-5} \text{ s}^{-1}$ . Dotted lines establish correspondence between the abrupt stress drops and the AE events. It can be seen that AE events with similar amplitude occur during both stress drops and smooth reloading periods. In the time interval shown in the figure, the two biggest AE events (marked by dotted lines) do not correspond to stress drops.

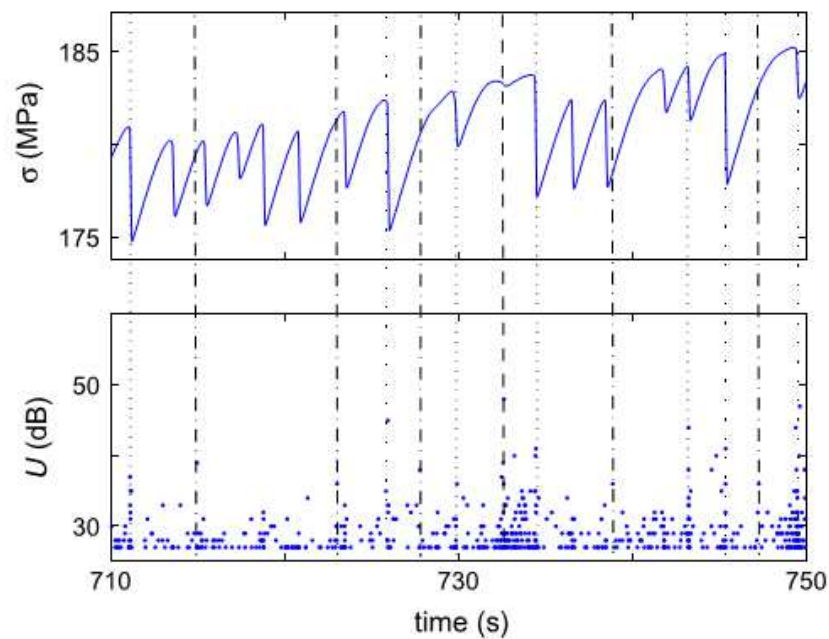


**Fig. 2.** Blow up of parts of a deformation curve  $\sigma(t)$  and the accompanying AE signal  $U(t)$  for  $\dot{\epsilon}_a = 2 \times 10^{-4} \text{ s}^{-1}$ . Dotted lines show the abrupt stress drops accompanied by AE burst events. The maximum burst in the time interval shown corresponds to a weak stress fluctuation, as marked by the dashed line. Bursts also occur during smooth reloading periods. Some (not all) of these bursts are shown by dash-dotted lines.

The analysis was performed over intervals  $T$  during which the aspect of both AE and the normalized stress fluctuations and their range of variation remain unchanged. In addition, the robustness of the analysis was verified by varying the boundaries of the interval and checking that the difference in the  $D_q$  values remains within the respective standard deviation estimated by the least squares method. The  $D_q$ -spectra were plotted by varying  $q$  in a large interval from -20 to 40. Recently, it was shown that the estimates of the scaling exponents systematically depart from the correct values for large  $q$ -numbers ( $|q| > 10$ ) [21]. Still, the corresponding curves are useful as sensitive indicators of any imperfectness of the linear trend. For this reason and because the present analysis is based on the relative changes occurring when either the experimental conditions or the scale of observation are varied, such data shall also be used in further illustrations.

#### 4. Experimental results

Multifractality of the deformation curves was found for all strain rates, and displayed behavior similar to that reported earlier [4,11,15–17]. Only the features necessary for comparison with AE behavior are presented below. Figs. 1 and 2 collate the stress serrations and the simultaneous records of the amplitudes of AE events for a low and an intermediate  $\dot{\epsilon}_a$  value, at which distinct stress serrations separated by smooth reloading are observed. It can be seen that AE events with amplitudes in a similar range occur both at the instants of the stress drops and during smooth deformation (cf. Ref. [13]). Fig. 3 presents the corresponding results of the MF analysis. For the deformation curves, fans of linear  $\log(S_q)$  vs.  $\log(\delta_t)$  dependences are found over intervals covering about an order of magnitude of  $\delta_t$ . The dependences deviate from straight lines and come close to constant when  $\delta_t$  is decreased and approaches the value corresponding to the minimum interval  $\Delta t_{min}$  between the abrupt stress drops. The upper scaling limit relates to the size of the series: the dependences tend towards the trivial value  $D_q = 1$  when  $\delta_t$  approaches the total interval  $T$ . The spectrum of generalized dimensions (further called MF spectrum) obtained using a family of such dependences for the specimen from Fig. 1 is displayed in Fig. 4 (open circles). In some cases the MF scaling is only revealed after removing small-amplitude events from the time series. The procedure consists in gradual truncation of small events until a smooth MF spectrum is obtained for the remaining data subset [16]. As discussed in Ref. [16], such behavior suggests that not all mobile dislocations are involved in the correlated process giving rise to multifractality of the time series, and that there are also uncorrelated events, seemingly among the least intensive ones.

Multifractal behavior was also found for the corresponding AE time series, except for the highest strain rate,  $\dot{\epsilon}_a = 6 \times 10^{-3} \text{ s}^{-1}$ . In this last case, a tendency to form fans of linear  $\log(S_q)$  vs.  $\log(\delta_t)$  dependences was also observed, but smooth MF spectra were not obtained, which is likely due to the decreasing capacity of the AE technique to resolve individual AE events when the overall AE activity increases. This is confirmed by control tests with different HDT settings, which showed enhanced (and dependent on the HDT) ranges of durations of the AE events at the highest strain rate (cf. Ref. [22]).

Significantly, the scaling range displayed by the partition functions found for the AE time series is much larger than that for the respective deformation curves, as can be seen in Fig. 3. The extension occurs through shifting the lower  $\delta_t$  limit to values considerably less than  $\Delta t_{min}$ . Importantly, the slope of the  $\log(S_q) - \log(\delta_t)$  dependences remains identical all over the interval and does not change when  $\delta_t$  falls in the range pertaining to smooth deformation. It can thus be conjectured that the AE events observed during jerky flow belong to the same multifractal ensemble, be they related to stress drops or to smooth deformation. Strictly speaking, low-amplitude events may be uncorrelated because, similarly to the case of the deformation curves, their truncation is sometimes needed to uncover the scaling. For example, whereas the dependences in Fig. 3b are obtained using all recorded events (that is, the events exceeding the threshold of 27 dB), those in Fig. 3a correspond to the events with the logarithmic amplitude above 34 dB. Similar to Ref. [16], it was checked that the truncation does not affect the slope of the multifractal partition functions.

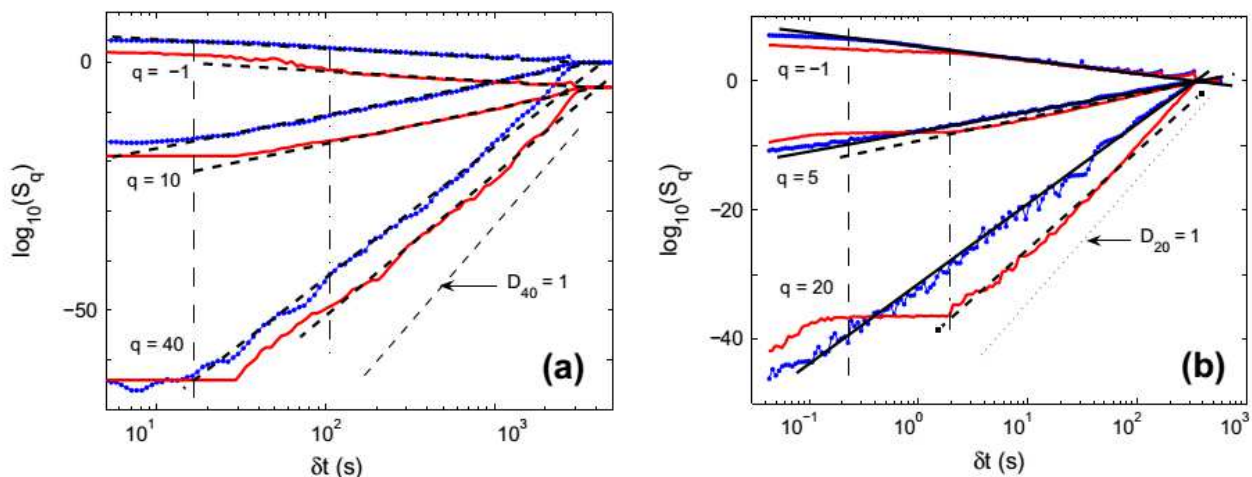


**Fig. 3.** Blow Comparison of partition function  $S_q(\delta t)$  for AE time series (lines with symbols) and for the stress time series (lines without symbols) for the specimens of Figs 1 and 2. (a)  $\dot{\epsilon}_a = 2 \times 10^{-5} \text{ s}^{-1}$ ;  $T = [10,000 \text{ s}; 13,000 \text{ s}]$ ; the family of lines without symbols is shifted downwards to improve the readability of the figure. (b)  $\dot{\epsilon}_a = 2 \times 10^{-4} \text{ s}^{-1}$ ;  $T = [650 \text{ s}; 1000 \text{ s}]$ . The numbers near the pairs of curves indicate the corresponding  $q$ -value. The vertical dashed lines indicate the lower scaling limit for AE; the vertical dash-and-dotted lines, for the stress time series. The line corresponding to the trivial scaling  $D_q = 1$  is shown for the maximum  $q$ -values. For the sake of readability, the curves for high negative  $q$ -values are not shown because of the high data scatter (cf. error bars in Fig. 4). This is typical of the analysis of real signals because these  $q$ -values correspond to the sparsely data subsets, which are mostly drowned in the experimental noise (cf. e.g. Ref. [4,]).

The slopes of the scaling dependences do not necessarily coincide for the AE and stress time series. The example in Fig. 3a displays a situation where both families of partition functions have close slopes and lead to the similar MF spectra presented in Fig. 4. The opposite example shown in Fig. 3b questions the above conclusion. The reason for such discrepancy will be discussed in the following.

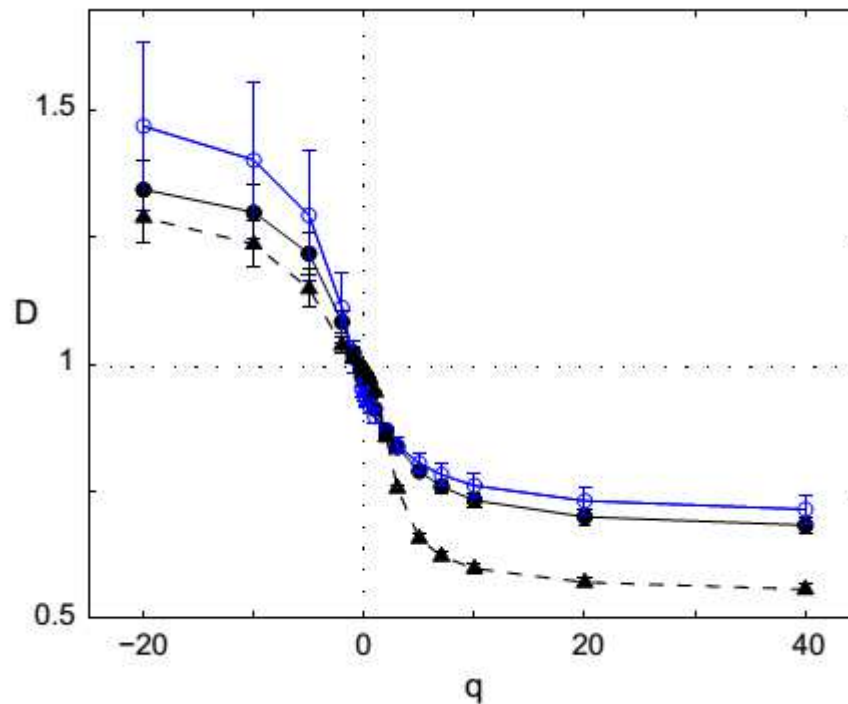


**Fig. 4.** Examples of spectra of generalized dimensions  $D_q$  for a portion of the deformation curve with stress serrations (open circles) and the corresponding AE signals (full circles).  $\dot{\epsilon}_a = 2 \times 10^{-5} \text{ s}^{-1}$  and  $T = [10,000 \text{ s}; 13,000 \text{ s}]$ . Triangles show the spectrum for the AE series in an interval below  $\epsilon_{cr}$ ;  $T = [4000 \text{ s}; 5870 \text{ s}]$  for the same applied strain rate  $\dot{\epsilon}_a = 2 \times 10^{-5} \text{ s}^{-1}$ .

The second substantial conclusion arising from this analysis is that MF spectra are also found for the AE observed during the macroscopically smooth plastic flow below  $\epsilon_{cr}$ , as illustrated in Fig. 4 (curve marked by triangles). This means that the correlations in the dislocation dynamics leading to the emergence of MF patterns exist before the occurrence of the strong self-organization effects, which are generally associated with macroscopic plastic instability.

To find an indication of whether the fractal behavior is controlled by variations in the amplitude of the events or their arrangement in time, we analyzed several surrogate time series. In some tests, the events amplitudes were kept unchanged but the intervals between the events were either replaced with random series or kept constant. This led to suppressing multifractality, as illustrated in Fig. 5. Alternatively, the occurrence times of the events were kept unchanged but their amplitudes were shuffled or replaced with random series, or with a constant value. The effect of these perturbations depends on the type of modification chosen but the resulting deterioration of the

scaling curves was weak (sometimes negligible) in all cases. It can therefore be suggested that the time correlations between plastic events prevail as to the emergence of a MF structure, while the amplitudes of the corresponding AE events appear to be weakly correlated. This conclusion is consistent with the generally accepted notion that the prevailing correlation mechanism between plastic events is the long-range internal stress field generated in a heterogeneously deforming material. It is of interest to note that a similar behavior of surrogate series was found in a recent model of collective motion of only several dislocations [23]. The weaker effect of the perturbation of the AE amplitudes on the MF spectra is consistent with discrete dislocation dynamics simulations [24], which indicate that the amplitude of the plastic events is influenced by short-range interactions with the local dislocation microstructure through dislocation reactions, immobilization, or multiplication, e.g. due to double cross-slip of dislocations. The observable, albeit slight, changes in the MF spectra upon amplitude modifications bear witness to the relevance of the short-range interactions in the interpretation of the self-organization of dislocation ensembles.

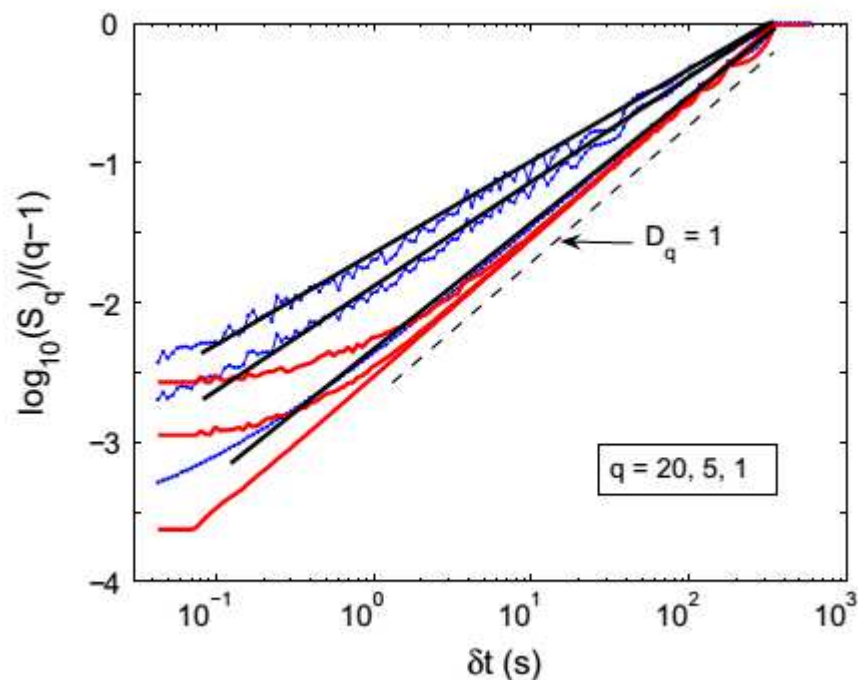


**Fig. 5.** Comparison of scaling for the original AE time series recorded at  $\dot{\epsilon}_a = 2 \times 10^{-4} \text{ s}^{-1}$  (lines with symbols) and for the surrogate data in which the real inter-event intervals are replaced with a random series (lines without symbols). The upper curve in each family corresponds to  $q = 20$ , the middle curve is obtained for  $q = 5$ , and the bottom curve for  $q = 1$ . For this sample, the dependences obtained when the intervals are kept unchanged and the amplitudes perturbed (see the text) almost coincide with the initial curves and are not shown.

Before launching the discussion section, it is worth specifying that although the trends described above are generally found in all tests, the spectra may visibly vary between samples deformed in the same conditions. In Ref. [4], such variations were conjecturally related to the sensitivity of the MF spectra to the material microstructure, which is obviously an important factor for the correlation of the dislocation dynamics. This conjecture is consistent with the present data.

Particularly, the variations from sample to sample were stronger at small strains. Consequently, no specific tendency was determined for the effect of strain rate on the MF spectra in this region, in conformity with the fast transformations of the dislocation microstructure usually induced by work-hardening upon the onset of plastic deformation. This qualitative observation finds confirmation in the comparison with the MF spectra at later stages of deformation in the same tests, as can be seen in Fig. 4. Indeed, the curve designated by triangles (small-strain interval) shows lower  $D_q$  values than the curve marked by full circles (large-strain interval), which testifies to a higher singularity of the AE series gathered at small strains. This is also consistent with the observation of a stronger and more irregular AE at the onset of plastic deformation, as reported in the literature (cf. Ref. [18]) and observed in the present experiments.

## 5. Discussion and conclusions

As was mentioned in the Introduction, various mechanisms of collective dislocation dynamics may be involved in the PLC effect, in spite of the ubiquitous presence of dislocation glide at microscopic scale. Since the abrupt stress drops reveal remarkably strong self-organization effects, this phenomenon is usually discussed apart from the self-organization occurring during smooth plastic flow [25]. The present data bear evidence that the difference in nature between the smooth and unstable plastic flow may be less substantial than it was believed, because the underlying processes are similar at the mesoscopic scale revealed by acoustic emission.

Three major results of the present study should indeed be emphasized. (i) Multifractality is found in series of AE events accompanying dislocation processes unresolved in mechanical testing, and is observed during both the initial smooth flow and the jerky flow occurring after a certain critical strain, which includes stress serrations and smooth reloading periods. (ii) The scaling ranges found for the AE observed during serrated flow overlap those for the corresponding stress–time series, and extend further over time scales shorter by an order of magnitude. As pointed out above, the multifractal character of AE is not a trivial consequence of the multifractality of the jerky stress–time series. It provides evidence for the similar nature of dislocation avalanches, whether they are associated with macroscopic stress serrations or smooth plastic flow. (iii) However, the observation of different scaling exponents for the two kinds of measurements indicates some differences in the nature of the dynamic regime, as seen from the macroscopic stress–time series or the mesoscopic AE signal. For a multifractal object, invoking a shift in the partition functions with the resolution coarsening to suggest that changes in the dynamical regime are indeed plausible, but additional arguments in favor of such differences follow from the comparison of the statistical distributions of stress drops and acoustic events amplitude [13]. As pointed out in the Introduction,

at high strain rates, scale-invariant (power-law) statistical distributions are observed for both ensembles, but the respective scaling exponents are also different. Even more conclusive is the fact that, at low and medium strain rates, peaked statistical distributions of the amplitude of stress drops are seen, whereas AE amplitudes are still characterized by scale-free statistics.

Hints at the explanation of the contrast between the mesoscale and macroscale observations may be found in the counter-intuitive behavior of the series of AE amplitudes. Indeed, the AE amplitude recorded at the instants of such powerful plastic events as the stress drops does not surpass that accompanying the smooth periods (cf. Figs. 1 and 2).<sup>1</sup> In contrast, higher order-of-magnitude bursts occur in the time series depending on the event duration, as commonly reported in the literature [13,18,19]. As indicated in Ref. [13], the concurrent absence of amplitude bursts and presence of duration bursts suggest that a PLC band does not occur due to the motion of larger-than-usual dislocation ensembles, but is formed instead through a process of synchronization of glide events of a similar amplitude range,<sup>2</sup> most probably triggered by the propagation of elastic waves. In particular, this synchronization assumption may explain the differences in the slopes of the partition functions for the stress and AE time series discussed above. Indeed, in contrast to a single dislocation avalanche, which can occur due to localized internal stresses, synchronizing several avalanches requires an overdriven system. This additional requirement may affect the correlation in time of the stress drops. Complementary experimental evidence of synchronization is provided by correlation and statistical analyses, which will be reported elsewhere.

Furthermore, the synchronization conjecture may contribute to the interpretations proposed earlier [4,27,28] to explain the above-mentioned crossover from peaked to power-law statistics of jerky flow with varying the driving strain rate [4]. As will be seen below, it is helpful in explaining why, at large applied strain rates, scale-free statistics is observed in both the mesoscopic and macroscopic time series (although different scaling exponents reflect different correlation mechanisms) and why, at low and medium strain rates, peaked distributions are seen at the macroscopic level while power-law behavior still prevails in the mesoscopic time series. According to the interpretations referred to above, little time is allowed at high strain rates for the plastic relaxation of internal stresses during the reloading periods between stress drops, which results in a high degree of spatial correlation. The system is “close” to accommodating the applied straining conditions through spatially uniform plastic strain rate, so that most dislocation ensembles are close

---

<sup>1</sup> This does not mean that the amplitudes of AE events are absolutely not correlated with the stress drops. Certain correlation is obvious in Fig. 2. Moreover, the quantitative analysis reveals (weak) correlation even for the data of Fig. 1. The rigorous correlation analysis goes beyond the scope of this paper and will be published elsewhere.

<sup>2</sup> The absence of larger AE amplitudes may be due to the natural cut-off in the size of the dislocation avalanches, the mechanisms of which are discussed, e.g., in Ref. [26]).

to the threshold for unpinning. As a consequence, dislocation avalanches can occur on any scale and at any time when triggered by propagating elastic fluctuations, which leads to scale-free distributions of stress drops. Thus synchronization of avalanches only plays a minor role in the transition from mesoscopic to macroscopic plastic events. As the applied strain rate is decreased, the system becomes increasingly overdriven, with a large part of the dislocation ensembles lying in a strongly pinned state. Therefore, accommodation of the imposed strain rate can only be achieved through large localized plastic deviations from the threshold of instability. According to the present results, these large events are due to the synchronization of standard-size dislocation avalanches at mesoscale, and not to unpinning of very large dislocation ensembles. Since plastic relaxation of internal stresses takes place during the reloading sequences, spatial correlations are weaker and the correlation distance is shorter than at high strain rates. Hence, the synchronized dislocation avalanches are more localized in space and time, and of a more typical and limited size. As discussed in Refs. [27,28], they will produce hopping bands associated with chaotic dynamics at medium strain rates when residual stresses are marginally relaxed, and randomly distributed bands at low strain rates when the residual stresses are fully relaxed.

Finally, it may be observed that the scale invariance reflected by the power-law statistics requires relatively weak pinning obstacles to dislocation motion, whereas an increased strength of obstacles, such that offered by dynamic strain aging, is needed for the occurrence of peaked event distributions [29]. Strong obstacles have the effect of shifting the dislocation ensembles away from the threshold for unpinning, and their dynamics from criticality. This feature is illustrated in Fig. 7 of Ref. [27] and Fig. 3 of Ref. [28], which show that most dislocations are close to the threshold of unpinning in the scaling regime, whereas in the chaotic regime a large fraction is in the pinned state. The results of this work show that, in the presence of strong obstacles, collective unpinning of dislocations occurs through synchronization of regular size dislocation avalanches, whereas synchronization is relatively ineffective in the presence of weak obstacles.

### **Acknowledgements**

This work was partly supported by the program of scientific exchanges between CNRS and the Russian Academy of Sciences (Project 23992). One of the authors (N.P.K) would like to acknowledge financial support from Region Lorraine for his visits to the University Paul Verlaine–Metz.

### **References.**

- [1] Lebyodkin MA, Brechet Y, Estrin Y, Kubin LP. *Phys Rev Lett*, 74 :4758, 1995

- [2] Ananthakrishna G, Fressengeas C, Grosbras M, Vergnol J, Engelke C, Plessing J, et al. *Scripta Metall Mater*, 32:1731, 1995
- [3] Ananthakrishna G, Noronha SJ, Fressengeas C, Kubin LP. *Phys Rev E*, 60:5455, 1999
- [4] Bharathi MS, Lebyodkin M, Ananthakrishna G, Fressengeas C, Kubin LP. *Acta Mater*, 50:2813, 2002
- [5] Sarkar A, Webber Jr CL, Barat P, Mukherjee P. *Phys Lett A*, 372:1101, 2008
- [6] Kugiumtzis D, Kehagias A, Aifantis EC, Neuhäuser H. *Phys Rev E*, 70:036110, 2004
- [7] Darowicki K, Orlikowski J, Zielinski A, Jurczak W. *Comput Mater Sci*, 39:880, 2007
- [8] Lebyodkin MA, Lebedkina TA, Chmelik F, Lamark TT, Estrin Y, Fressengeas C, et al. *Phys Rev B*, 79:174114, 2009
- [9] Bak P, Tang C, Wiesenfeld V. *Phys Rev A*, 38:364, 1988
- [10] Abarbanel HDI, Brown R, Sidorowich JJ, Tsimring LSh. *Rev Mod Phys*, 65:133, 1993
- [11] Lebyodkin MA, Estrin Y. *Acta Mater*, 53:3403, 2005
- [12] Richeton T, Dobron P, Chmelik F, Weiss J, Louchet F. *Mat Sci Eng A*, 424:190, 2006
- [13] Bougherira Y, Entemeyer D, Fressengeas C, Kobelev NP, Lebedkina TA, Lebyodkin MA. *J Phys: Conf Series*, 240:012009, 2010
- [14] Dimiduk DM, Woodward C, LeSar R, Uchic MD. *Science*, 312:1188, 2006
- [15] Lebyodkin MA, Lebedkina TA. *Phys Rev E*, 73:036114, 2006
- [16] Lebyodkin MA, Lebedkina TA. *Phys Rev E*, 77:026111, 2008
- [17] Lebedkina TA, Lebyodkin MA. *Acta Mater*, 56:5567, 2008
- [18] Chmelik F, Ziegenbein A, Neuhauser H, Lukac P. *Mater Sci Eng A*, 324:200, 2002
- [19] Kumar J, Ananthakrishna G. *Phys Rev Lett*, 106:106001, 2011
- [20] Halsey TC, Jensen MH, Kadanoff LP, Procaccia I, Shraiman BI. *Phys Rev A*, 33:1141, 1986
- [21] Lashermes B, Abry P. *Int J Wavelets*, 2:497, 2004
- [22] Bougherira Y. PhD report. Université Paul Verlaine-Metz: Metz, 2011
- [23] Li R, Picu RC, Weiss J. *Phys Rev E*, 82:022107, 2010

- [24] Devincre B, Hoc T, Kubin L. *Science*, 320:1745, 2008
- [25] Zaiser M. *Adv Phys*, 55:185, 2006
- [26] Weiss J, Richeton T, Louchet F, Chmelik F, Dobron P, Entemeyer D, et al. *Phys Rev B*, 76:224110, 2007
- [27] Kok S, Bharathi MS, Beaudoin AJ, Fressengeas C, Ananthakrishna G, Kubin LP, et al. *Acta Mater*, 51:3651, 2003
- [28] Bharathi MS, Ananthakrishna G. *Phys Rev E*, 67:065104, 2003
- [29] Ananthakrishna G, Fressengeas C. *Scripta Mater*, 52:425, 2005